

MODEL-CONSTRAINED DEEP LEARNING APPROACHES FOR INVERSE PROBLEMS*

HAI V. NGUYEN[†] AND TAN BUI-THANH[‡]

Abstract. Deep Learning (DL), in particular deep neural networks (DNN), by design is purely data-driven and in general does not require physics. This is the strength of DL but also one of its key limitations when applied to science and engineering problems in which underlying physical properties—such as stability, conservation, and positivity—and desired accuracy need to be achieved. DL methods in their original forms are not capable of respecting the underlying mathematical models or achieving desired accuracy even in big-data regimes. On the other hand, many data-driven science and engineering problems, such as inverse problems, typically have limited experimental or observational data, and DL would overfit the data in this case. Leveraging information encoded in the underlying mathematical models, we argue, not only compensates missing information in low data regimes but also provides opportunities to equip DL methods with the underlying physics and hence obtaining higher accuracy. This short communication introduces several model-constrained DL approaches—including both feed-forward DNN and autoencoders—that are capable of learning not only information hidden in the training data but also in the underlying mathematical models to solve inverse problems. We present and provide intuitions for our formulations for general nonlinear problems. For linear inverse problems and linear networks, the first order optimality conditions show that our model-constrained DL approaches can learn information encoded in the underlying mathematical models, and thus can produce consistent or equivalent inverse solutions, while naive purely data-based counterparts cannot.

Key words. Inverse problem, optimization, model-constrained, deep learning, deep neural network.

1. Introduction. Inverse problems are pervasive in scientific discovery and decision making for complex, natural, engineered, and societal systems. They are perhaps the most popular mathematical approaches for *enabling predictive scientific simulations* that *integrate observational/experimental data, simulations and/or models* [27, 16, 39]. Many engineering and sciences systems are governed by parametrized partial differential equations (PDE). Computational PDE-constrained inverse problems faces not only the ill-posed nature—namely, non-existence, non-uniqueness, instability of inverse solutions—but also the computational expense of solving the underlying PDEs. Computational inverse methods typically require the PDEs to be solved at many realizations of parameter and the cost is an (possibly exponentially) increasing function of the parameter dimension. The fast growth of this cost is typically associated with the curse of the dimensionality. Inverse problems for practical complex systems [1, 27, 18, 5, 20] however possess this high dimensional parameter space challenge. Thus, mitigating the cost of repeatedly solving the underlying PDE has been of paramount importance in computational PDE-constrained inverse problems.

The field of Machine Learning (ML) typically refers to computational and statisti-

*The first version of work was an Oden Institute technical report 21-09, May 11, 2021, and then presented at the Uncertainty Quantification and Probabilistic Modeling Technical Thrust Area, US-NCCM, May 17, 2021.

Funding: This work was partially funded by the National Science Foundation awards NSF-1808576 and NSF-CAREER-1845799; by the Defense Thread Reduction Agency award DTRA-M1802962; by the Department of Energy award DE-SC0018147; and by 2020 ConTex award; and by 2018 UT-Portugal CoLab award.

[†]Department of Aerospace Engineering and Engineering Mechanics, the University of Texas at Austin, Texas (hainguyen@utexas.edu)

[‡]Department of Aerospace Engineering and Engineering Mechanics, The Oden Institute for Computational Engineering and Sciences, the University of Texas at Austin, Texas (tanbui@oden.utexas.edu, <https://users.oden.utexas.edu/~tanbui/>).

cal methods for automated detection of meaningful patterns in data [2, 36, 26]. While Deep Learning (DL) [11], a subset of machine learning, has proved to be state-of-the-art methods in many fields of computer sciences such as computer vision, speech recognition, natural language processing, etc, its presence in the scientific computing community is, however, mostly limited to off-the-shelf applications of deep learning. Unlike classical scientific computational methods, such as finite element methods [7, 4, 9], in which solution accuracy and reliability are guaranteed under regularity conditions, standard DL methods are often far from providing reliable and accurate predictions for science and engineering applications. The reason is that though approximation capability of deep learning, e.g. via Deep Neuron Networks (DNN), is as good as classical methods in approximation theory [8, 13, 24, 15], DL accuracy is hardly attainable in general due to limitation in training. It has been shown that the training problem is highly nonlinear and non-convex, and that the gradient of loss functions can explode or vanish [12], thus possibly preventing any gradient-based optimization methods from reliably converging to a minimizer. Even when converged, the prediction of the (approximate) optimal deep learning model can be prone to over-fitting and can have poor generalization error.

Many data-driven inverse problems in science and engineering problems have limited experimental or observational data, e.g. due to the cost of placing sensors (e.g. digging an oil well can cost million dollars) or the difficulties of placing sensors in certain regions (e.g. deep ocean bottoms). DL, by design, does not require physics, but data. This is the strength of DL. It is also the key limitation to science and engineering problems in which underlying physics need to be respected (e.g. stability, conservation, positivity, etc) and higher accuracy is required. In this case, purely data-based DL approaches are prone to over-fitting and thus incapable of respecting the physics or providing desired accuracy. Similar to least squares finite element methods [3], we can train a DNN solution constrained by the PDE residual as a regularization [35, 31, 33, 34, 42, 40, 22, 28]). The resulting physics-informed DNN (PINN) models can learn solutions that attempt to make the PDE residual small. The PINN approach directly approximates the PDE solution in infinite dimensional spaces. While universal approximation results (see, e.g., [8, 13, 24, 15]) could ensure any desired accuracy with sufficiently large number of neurons, practical network architectures are moderate in both depth and width, and hence the number of weights and biases. Therefore, the accuracy of PINN can be limited.

Moreover, for *parametrized PDEs*—that are pervasive in design, control, optimization, inference, and uncertainty quantification—training a PINN together with parameters (either by themselves or their neural networks weights and biases as another set of optimization variables) [6, 32, 22, 23] may not be efficient as new observational data (corresponding to new unknown parameters) requires a retraining. It is also not clear how to extend the current PINN inversion strategy to statistical inverse problems. We note that attempts using pure data-driven deep learning to learn the parameter to observable map have been explored (see, e.g., [17, 41, 29, 38, 30, 17, 37, 14]). Approaches using autoencoder spirit that train a forward network first and then an inverse network in tandem [21, 25] or both of them simultaneously [10] have also proposed. While successes are reported, generalization capability, and hence success, could be limited to regimes seen in the training data as the governing equations—containing most, if not all, information about the underlying physics—are not involved in the training.

For inverse problems, the object of interest is not the solution of parametrized PDE, per say, but some observable integrated Quantity of Interest (QoI) of the solution. Since the solution depends on the parameter, QoI is a function of parameter.

The mapping from parameter to some observable QoI is known as the parameter-to-observable map. Unlike the solution, QoI does not depend on spatial or temporal variables but only on the parameter. Moreover, for most of engineering and sciences application the dimension of QoI or observational data is typically much less than that of the solution. Thus, massive information about spatial, temporal, and parameter is squashed into a small and/or finite observational data. Learning the parameter-to-observable map, we argue, is thus much less challenging [19].

The paper is organized as follows. Notations are described in [section 2](#). In [section 3](#) we briefly introduce nonlinear inverse problems, and a data-driven naive DNN (nDNN) approach, and its solution for linear network with one layer and linear inverse problem are presented. The goal of [section 4](#) is to present a model-constrained DNN (MCDNN) approach designed to learn the inverse map while being constrained by the parameter-to-observable map of the underlying discretized PDE. Then, we present two model-constrained decoder approaches to learn the inverse map in [section 5](#) and a model-constrained encoder approach in [section 6](#). We conclude the paper with future research directions in [section 8](#).

2. Notations.

- Boldface lower cases are for (column) vectors.
- Uppercase letters are for matrices. I is the identity matrix, whose size is clear from the context in which it appears.
- \mathbf{u} is the vector of parameters in the underlying parametrized PDEs.
- \mathbf{w} is the solution of the underlying parametrized PDEs.
- $\boldsymbol{\theta}$ is the vector of all weights and biases of DNN.
- \mathcal{G} denotes general nonlinear parameter-to-observable or forward map.
- G is preserved to denote a linear parameter-to-observable or forward map.
- \mathbf{y} denotes the vector observational data or quantity of interest.
- n_t is the number of training scenarios/data.
- m is dimension (number of rows) of the parameter vector \mathbf{u} .
- n is dimension (number of rows) of each observable data vector \mathbf{y} .
- $U \in \mathbb{R}^{m \times n_t}$ is the parameter matrix concatenating available parameter \mathbf{u} .
- $Y \in \mathbb{R}^{n \times n_t}$ is the data matrix concatenating available data \mathbf{y} .
- $\{U, Y\}$ or $\{Y, U\}$ is the training data set.
- Γ is the covariance matrix of parameter prior.
- Λ is the covariance matrix of additive noise added to data \mathbf{y} .
- $\mathbf{1} \in \mathbb{R}_t^n$ is the column vector with all ones.
- $\|\cdot\|$ denotes standard Euclidean norm for vectors and Frobenius norm for matrices.

3. Forward and inverse problems. We denote by $\mathbf{u} \in \mathbb{R}^m$ the parameters sought in the inversion, by $\mathbf{w} \in \mathbb{R}^s$ the forward states, by $\mathcal{G} : \mathbb{R}^s \rightarrow \mathbb{R}^n$ the forward map (computing some observable quantity of interest), and by $\mathbf{y} \in \mathbb{R}^n$ the observations. For the clarity of the exposition, we assume there is no observation noise or error, thus

$$(3.1) \quad \mathbf{y} := \mathcal{G}(\mathbf{w}(\mathbf{u})).$$

The parameter-to-observable (PtO) map is the composition of the forward map \mathcal{G} and the states, i.e. $\mathcal{G} \circ \mathbf{w}$. However for simplicity of the exposition, we do not distinguish it from the forward map and thus we also write $\mathcal{G} : \mathbb{R}^m \ni \mathbf{u} \mapsto \mathcal{G}(\mathbf{u}) := \mathcal{G}(\mathbf{w}(\mathbf{u})) \in \mathbb{R}^n$.

The forward state is the solution of the forward equation

$$(3.2) \quad \mathcal{F}(\mathbf{u}, \mathbf{w}) = \mathbf{f}.$$

Assume that (3.2) is well-posed so that, for a given set of parameters \mathbf{u} , one can (numerically for example) solve for the corresponding forward states $\mathbf{w} = \mathbf{w}(\mathbf{u}) := \mathcal{F}^{-1}(\mathbf{f})$. In the forward problem, we compute observational data \mathbf{y} via (3.1) given a set of parameter \mathbf{u} . In the inverse problem, we seek to determine the unknown parameter \mathbf{u} given some observational data \mathbf{y} , that is, we wish to construct the inverse of \mathcal{G} . Since m is typically (much) larger than n for many practical problems, the parameter-to-observable map \mathcal{G} is not invertible even when \mathcal{G} is linear. The inverse task is thus ill-posed and notoriously challenging as a solution for \mathbf{u} may not exist (non-existence), even when it may, it is not unique (non-uniqueness) nor continuously depends on the data \mathbf{y} (instability). An approximate solution is typically sought via (either deterministic or statistical) regularization.

Given the popularity of the emerging machine learning, in particular deep neural networks (DNN), methods, we may attempt to apply pure data-driven DNN, or naive DNN (nDNN), to learn the (ill-posed) inverse of \mathcal{G} , e.g.,

$$(nDNN) \quad \min_{\mathbf{b}, W} \frac{1}{2} \|U - \Psi(Y, W, \mathbf{b})\|^2 + \frac{\alpha_1}{2} \|W\|^2 + \frac{\alpha_2}{2} \|\mathbf{b}\|^2,$$

where Ψ is a DNN with weight matrix W and bias vector \mathbf{b} and the last two terms are regularizations for weights and biases with nonnegative regularization parameters α_1 and α_2 . This approach completely disregards the underlying mathematical model (3.1)-(3.2). In particular, even for linear inverse problem—for example, $\mathcal{G}(\mathbf{u}) = G\mathbf{u}$ and there is no error in computing the data so that $Y = GU$ —and linear DNN, it is not clear if the nDNN approach (nDNN) could recover a sensible solution of the original inverse problem

$$(3.3) \quad \min_{\mathbf{u}} \|\mathbf{y}^{obs} - G\mathbf{u}\|^2$$

in an interpretable sense. Indeed, suppose that we choose a linear activation function and one hidden layer such that the DNN model $\Psi(Y, W, \mathbf{b})$ for learning the inverse map can be written as $WY + B$, where $B := \mathbf{b}\mathbf{1}^T$. It is easy to see that the optimal weight W^0 and bias \mathbf{b}^0 for (nDNN) is given as

$$\begin{aligned} W^0 &= U \left(I - \frac{1}{n_t + \alpha_2} \mathbf{1}\mathbf{1}^T \right) Y^T \left[Y \left(I - \frac{1}{n_t + \alpha_2} \mathbf{1}\mathbf{1}^T \right) Y^T + \alpha_1 I \right]^\dagger \\ \mathbf{b}^0 &= \frac{1}{1 + \alpha_2/n_t} (\bar{\mathbf{u}} - W^0 \bar{\mathbf{y}}), \end{aligned}$$

where $\bar{\mathbf{u}} := \frac{1}{n_t} U\mathbf{1}$. Thus the nDNN inverse solution for a given testing/observational data \mathbf{y}^{obs} is given by

$$(3.4) \quad \mathbf{u}^{nDNN} = W^0 \mathbf{y}^{obs} + \mathbf{b}^0.$$

It is not clear if the nDNN inverse solution (3.4) provides an approximate solution to the original inverse problem (3.3) in an interpretable sense. This is a disadvantage of purely data driven approaches for science and engineering problems.

The data driven nature of DNN could be claimed as an advantage. However, DNN can be seen as an “interpolation” method and thus can generalize well only for scenarios that have been seen in or are closed to the training data set $\{U, Y\}$. This implies a possible enormous amount of training data to learn the inverse of a highly nonlinear forward model (3.1)-(3.2). In practical sciences and engineering problems, this extensive data regime is unfortunately rarely the case due to the high cost of placing sensors or the difficulties in placing sensors in certain regions. *In order for a DNN to generalize well in insufficient/low data regimes, we argue, it should be equipped with information encoded in the forward model (3.1)-(3.2) that is not covered in the data set.* In other words, it is natural to require DNN to be aware of the underlying mathematical models (or discretizations) in order for it to be a reliable and meaningful tool for sciences and engineering applications. *Such a physics encoding also supplies meaningful interpretations to DNN inverse solutions as we shall show.* The question is how to inform DNN about the underlying models?

In the following, as an effort to train DNN to learn not only information hidden in the training data but also complementary information in the underlying models, we explore several model-trained DNN approaches to learning the inverse of the PtO map \mathcal{G} . Though the approaches are designed for general nonlinear problems, our focus here is on linear PtO maps as this provides insights into if learning the inverse map via model-constrained DNN is at all possible, and if model-constrained DNN solution is potentially interpretable.

4. Model-Constrained Deep Neural Network (mcDNN) for learning the inverse map. We propose to learn the inverse map via DNN constrained by the forward map as

$$(mcDNN) \quad \min_{\mathbf{b}, W} \frac{1}{2} \|U - \Psi(Y, W, \mathbf{b})\|_{\Gamma^{-1}}^2 + \frac{\alpha}{2} \|Y - \mathcal{G}(\Psi(Y, W, \mathbf{b}))\|_{\Lambda^{-1}}^2,$$

where Ψ is a DNN learning the map from observable data \mathbf{y} to parameter \mathbf{u} with weight matrix W and bias vector \mathbf{b} . Unlike the naive purely data-driven DNN approach (nDNN), the model-constrained (mcDNN) makes the DNN Ψ aware that the training data is generated by the forward map \mathcal{G} . This is done by requiring the output of the DNN—approximate unknown parameter \mathbf{u} for a given data \mathbf{y} as the input—when pushed through the forward model \mathcal{G} , reproduces the data \mathbf{y} . The model-aware term $\frac{\alpha}{2} \|Y - \mathcal{G}(\Psi(Y, W, \mathbf{b}))\|_{\Lambda^{-1}}^2$ can be considered as a physics-informed regularization approach for mcDNN (compared to the non-physical regularizations in (nDNN)).

To provide some intuition for our mcDNN approach let us choose a linear activation function such that the one-layer DNN model $\Psi(Y, W, \mathbf{b})$ for leaning the inverse map can be written as $WY + B$, where $B := \mathbf{b}\mathbf{1}^T$. We also assume that the forward map is linear. For linear inverse problem with linear DNN, the model-constrained training problem (mcDNN) becomes

$$(4.1) \quad \min_{\mathbf{b}, W} \frac{1}{2} \|U - (WY + B)\|_{\Gamma^{-1}}^2 + \frac{\alpha}{2} \|Y - \mathcal{G}(WY + B)\|_{\Lambda^{-1}}^2.$$

LEMMA 4.1. *The optimal solution W^I and \mathbf{b}^I of the DNN training problem (4.1)*

satisfies

$$\begin{aligned}\mathbf{b}^I &= (\Gamma^{-1} + \alpha G^T \Lambda^{-1} G)^{-1} \left[\Gamma^{-1} \bar{\mathbf{u}} + \alpha G^T \Lambda^{-1} \bar{\mathbf{y}} - \left(\Gamma^{-1} \bar{U} \bar{Y}^\dagger + \alpha G^T \Lambda^{-1} \bar{Y} \bar{Y}^\dagger \right) \bar{\mathbf{y}} \right], \\ W^I &= (\Gamma^{-1} + \alpha G^T \Lambda^{-1} G)^{-1} \left[\Gamma^{-1} \bar{U} \bar{Y}^\dagger + \alpha G^T \Lambda^{-1} \bar{Y} \bar{Y}^\dagger \right],\end{aligned}$$

where $\bar{\mathbf{u}} := \frac{1}{n_t} U \mathbf{1}$ and $\bar{\mathbf{y}} := \frac{1}{n_t} Y \mathbf{1}$ are the column-average of the training parameters and data, $\bar{Y} := Y - \bar{\mathbf{y}} \mathbf{1}^T$, and $\bar{U} := U - \bar{\mathbf{u}} \mathbf{1}^T$.

COROLLARY 4.2. *For a given testing/observational data \mathbf{y}^{obs} , the mcDNN inverse solution \mathbf{u}^{mcDNN} of (4.1) is given by*

$$\begin{aligned}\mathbf{u}^{mcDNN} &= (\Gamma^{-1} + \alpha G^T \Lambda^{-1} G)^{-1} \\ &\quad \left[\Gamma^{-1} \bar{\mathbf{u}} + \alpha G^T \Lambda^{-1} \bar{\mathbf{y}} + \left(\Gamma^{-1} \bar{U} \bar{Y}^\dagger + \alpha G^T \Lambda^{-1} \bar{Y} \bar{Y}^\dagger \right) (\mathbf{y}^{obs} - \bar{\mathbf{y}}) \right]\end{aligned}$$

which is exactly the solution of the following regularized linear inverse problem

$$\min_{\mathbf{u}} \frac{1}{2} \|\mathbf{y}^{obs} - G\mathbf{u}\|_{\Lambda^{-1}}^2 + \frac{1}{2\alpha} \|\mathbf{u} - \mathbf{u}_0\|_{\Gamma^{-1}}^2,$$

where

$$\mathbf{u}_0 = \bar{\mathbf{u}} + \bar{U} \bar{Y}^\dagger (\mathbf{y}^{obs} - \bar{\mathbf{y}}) - \alpha \Gamma G^T \Lambda^{-1} (I - \bar{Y} \bar{Y}^\dagger) (\mathbf{y}^{obs} - \bar{\mathbf{y}}).$$

The results of [Corollary 4.2](#) shows that the mcDNN inverse solution \mathbf{u}^{mcDNN} is equivalent to a Tikhonov-regularized inverse solution with a data-informed reference parameter \mathbf{u}_0 that depends on the training set $\{U, Y\}$ and the given observational data \mathbf{y}^{obs} . In other words, *the model-constrained deep learning mcDNN approach is interpretable in the sense that it provides data-informed Tikhonov-regularized inverse solutions*.

5. Model-Constrained Decoder (mcDecoder) for learning the inverse map. Let us denote by $\Psi_e(\cdot, W_e, \mathbf{b}_e)$ the encoder with weight matrix W_e and bias vector \mathbf{b}_e , and by $\Psi_d(\cdot, W_d, \mathbf{b}_d)$ the decoder with weight matrix W_d and bias vector \mathbf{b}_d . We wish to train a model-constrained decoder (mcDecoder) in the following sense

$$\begin{aligned}(\text{mcDecoder}) \quad &\min_{\mathbf{b}_e, W_e, \mathbf{b}_d, W_d} \frac{\alpha}{2} \|Y - \Psi_e(U, W_e, \mathbf{b}_e)\|^2 + \\ &\frac{1}{2} \|U - \Psi_d(\Psi_e(U, W_e, \mathbf{b}_e), W_d, \mathbf{b}_d)\|^2 + \frac{\beta}{2} \|Y - \mathcal{G}(\Psi_d(\Psi_e(U, W_e, \mathbf{b}_e), W_d, \mathbf{b}_d))\|^2,\end{aligned}$$

where the first term forces the encoder to map the parameter \mathbf{u} to observation \mathbf{y} . The second term requires the decoder, after taking the encoder output as its input, reproduce the parameter. The third term is to ensure that the autoencoder system cannot be arbitrary but to obey the forward map. That is, the output of the decoder (which approximates the parameter), after going through the underlying forward map, must reproduce the data. Thus, *unlike standard autoencoder approach which is purely data-driven, our proposed autoencoder has the parameter as its input, the observational data as its latent variable, and its output aware of the forward map \mathcal{G}* . For linear NN and linear inverse problem, the mcDecoder formulation (mcDecoder) reduces to

$$\begin{aligned}(5.1) \quad &\min_{\mathbf{b}_e, W_e, \mathbf{b}_d, W_d} \frac{1}{2} \|U - W_d(W_e U + B_e) - B_d\|_F^2 + \frac{\alpha}{2} \|Y - W_e U - B_e\|_F^2 + \\ &\frac{\beta}{2} \|Y - G W_d(W_e U + B_e) - G B_d\|_F^2,\end{aligned}$$

where $B_e := \mathbf{b}_e \mathbf{1}^T$ and $B_d := \mathbf{b}_d \mathbf{1}^T$.

DEFINITION 5.1 (Equivalent inverse solution). *An inverse solution $\hat{\mathbf{u}}$ is equivalent to the true underlying parameter \mathbf{u}^* if*

$$\mathcal{G}(\hat{\mathbf{u}}) = \mathcal{G}(\mathbf{u}^*).$$

LEMMA 5.2. *The following combination*

$$\mathbf{b}_e^H = 0, \quad \mathbf{b}_d^H = 0, \quad W_e^H = G, \quad \text{and } W_d^H G = I,$$

is a stationary point of the lost function in the mcDecoder formulation (5.1).

That is, for this stationary point, the encoder weight matrix W_e^H in Lemma 5.2 is exactly the forward map G and the decoder weight matrix W_d^H is a left inverse of the forward map. In this case, given a new data \mathbf{y}^{obs} , it is easy to see that the decoder returns an equivalent inverse solution.

Next, let us consider a variant of (mcDecoder) given as

$$\begin{aligned} (\text{mcDecoderVar}) \quad \min_{\mathbf{b}_e, W_e, \mathbf{b}_d, W_d} J := & \frac{1}{2} \|U - \Psi_d(\Psi_e(U, W_e, B_e), W_d, B_d)\|^2 + \\ & \frac{\beta}{2} \|\Psi_e(U, W_e, B_e) - \mathcal{G}(\Psi_d(\Psi_e(U, W_e, B_e), W_d, B_d))\|^2, \end{aligned}$$

which, for linear neural network and linear inverse problem, becomes

$$\begin{aligned} (5.2) \quad \min_{\mathbf{b}_e, W_e, \mathbf{b}_d, W_d} J := & \frac{1}{2} \|U - W_d(W_e U + B_e) - B_d\|^2 + \\ & \frac{\beta}{2} \|W_e U + B_e - G W_d(W_e U + B_e) - G B_d\|^2, \end{aligned}$$

LEMMA 5.3. *The following combination*

$$\mathbf{b}_e^H = \mathcal{N}(W_d^H), \quad \mathbf{b}_d^H = 0, \quad G \times W_d^H = I, \quad \text{and } W_e^H \times W_d^H = I,$$

is a stationary point of the lost function in the mcDecoder formulation (5.2). Here, $\mathcal{N}(\cdot)$ denotes the null space. This is the unique optimal solution if, in addition, U and $W_d^H U$ have full row rank.

Lemma 5.3 shows that at the stationary point, the decoder weight matrix W_d^H is a right inverse for both the forward map G and the encoder weight matrix W_e^H . In addition, if the data is sufficient rich, this stationary point is the only optimal solution.

DEFINITION 5.4 (Consistent inverse solution). *An inverse solution $\hat{\mathbf{u}}$ is consistent if it reproduces the data \mathbf{y}^{obs} when pushed through the forward map \mathcal{G} , i.e.,*

$$\mathcal{G}(\hat{\mathbf{u}}) = \mathbf{y}^{obs}.$$

It is easy to see that the trained decoder in Lemma 5.3 provides consistent inverse solutions.

Remark 5.5. Since we are interested in the inverse solution or the decoder Ψ_d , designed in (mcDecoder)–(mcDecoderVar) as an approximate inverse map, is the primary object of interest. Should approximating the forward map $\mathcal{G}(\mathbf{u})$ be also desirable (such as for forward propagation of uncertainty), the encoder $\Psi_e(\cdot, W_e, \mathbf{b}_e)$,

once trained, can be used as an approximate forward map. In fact for linear inverse problems and linear neural networks, [Lemma 5.2](#) shows that the encoder could exactly learn the forward map in formulation [\(mcDecoder\)](#) while [Lemma 5.3](#) shows that the encoder could indirectly learn (since the decoder is a right inverse for both the forward map G and the encoder weight matrix W_e^{II}) the forward map in formulation [\(mcDecoderVar\)](#).

6. Model-constrained Encoder ([mcEncoder](#)) for learning the inverse map. \blacksquare

Recall in [section 5](#) we train the decoder to learn the inverse map. The training is regularized by requiring the encoder to behave similar to the forward map. In this section, we reverse the autoencoder structure, that is, we train the encoder to learn the inverse map and the training is regularized by requiring the decoder to behave like the forward map. Similar to [\(mcDecoder\)](#) we wish to train a model-constrained encoder by solving the following optimization problem.

$$\begin{aligned} (\text{mcEncoder}) \quad \min_{\mathbf{b}_e, W_e, \mathbf{b}_d, W_d} & \frac{\alpha}{2} \|U - \Psi_e(Y, W_e, B_e)\|^2 + \\ & \frac{1}{2} \|Y - \Psi_d(\Psi_e(Y, W_e, B_e), W_d, B_d)\|^2 + \frac{\beta}{2} \|Y - \mathcal{G}(\Psi_e(Y, W_e, B_e))\|^2, \end{aligned}$$

where the first term forces the decoder, as a surrogate to the inverse map, to transform observation \mathbf{y} to parameter \mathbf{u} . The second term requires the decoder, after taking the encoder output as its input, reproduces the observation. The third term is to ensure that the autoencoder system cannot be arbitrary but be constrained by the underlying forward map. That is, the output of the encoder (which approximates the unknown parameter), after going through the forward map, must reproduce the data. For linear NN and linear inverse problem, the [mcEncoder](#) formulation [\(mcEncoder\)](#) becomes

$$\begin{aligned} (6.1) \quad \min_{\mathbf{b}_e, W_e, \mathbf{b}_d, W_d} & J := \frac{1}{2} \|Y - W_d(W_e Y + B_e) - B_d\|_F^2 + \frac{\alpha}{2} \|U - W_e Y - B_e\|_F^2 + \\ & \frac{\beta}{2} \|Y - G W_e Y - G B_e\|_F^2, \end{aligned}$$

THEOREM 6.1. *At least one combination $W_e^{III}, \mathbf{b}_e^{III}, W_d^{III}$, and \mathbf{b}_d^{III} satisfying*

$$\begin{aligned} \mathbf{b}_e^{III} &= \bar{\mathbf{u}} - W_e^{III} \bar{\mathbf{y}}, \\ \mathbf{b}_d^{III} &= \bar{\mathbf{y}} - W_d^{III} \bar{\mathbf{u}}, \\ W_e^{III} &= W_e^{III} W_d^{III} W_e^{III}, \\ W_e^{III} &= W_e^{III} G W_e^{III}. \end{aligned}$$

is a stationary point of the optimization problem (6.1). In addition, if Y has full row rank, all stationary points, including optimal solutions, obey the above four identities. Clearly, any (W_e^{III}, W_d^{III}) satisfying

$$\begin{aligned} G W_e^{III} &= I, \\ W_d^{III} W_e^{III} &= I. \end{aligned}$$

is also a valid stationary point of (6.1).

Theorem 6.1 says that, once trained, the encoder weight matrix W_e^{III} of the mcEncoder formulation (6.1) can have the forward map G as its generalized inverse and the decoder weight matrix W_d^{III} behaves similar to the forward map in the sense that both are generalized inverses of W_e^{III} . In particular, this holds true at optimal solutions when the data is sufficiently rich, i.e., Y has full row rank. Again, this is not an entirely impractical assumption as the number of rows (n) of Y is typically much smaller than the number of rows (m) of U . **Theorem 6.1** also indicates that the encoder weight matrix W_e^{III} being a right inverse of the forward map G and the decoder weight matrix W_d^{III} is a favorable possibility. In this case, we have

$$G(W_e^{\text{III}}\mathbf{y}^{\text{obs}} + \mathbf{b}_e^{\text{III}}) = \mathbf{y}^{\text{obs}} = Gu^*,$$

which shows that the encoder is an approximate inverse map whose inverse solution is consistent as it exactly reproduces the observation \mathbf{y}^{obs} when pushed through the forward map.

7. Numerical results.

7.1. 1D linear deconvolution. We first analyze the 1D deconvolution to show the meaning of physic term in the linear inverse problem. In this problem, the linear operator G is Gaussian blurring kernel. To draw the training data set, we assume that our parameter is either the Dirichlet boundary or relaxed boundary first-order finite element matrix with prior mean

$$p_0 = 10(t - 0.5) \exp(-50(t - 0.5)^2) - 0.8 + 1.6t.$$

We mesh the domain $[0, 1]$ with 200 grid points which is the dimension of parameter. Meanwhile, we take randomly 10 observation points with 5% additive noise. The training data set size varies from 30 to 150, the fixed test data set is 50 in size. For each training data size, we average the relative error over 100 cases. The comparison of relative error between nDNN, mcDNN without covariance prior matrix norm, mcDNN and traditional inverse solver for Dirichlet boundary prior is shown in figure 1 and 2. Similarly, the figure 3 and 4 present the relative error for Relax boundary prior case.

Furthermore, in the case the training data size is very large, all methods tend to converge to the classical inverse solution for both cases of parameter prior, shown in the figure 5.

8. Conclusions. We argue that in order for a DNN to generalize well in insufficient data regimes, it should be equipped with information encoded in the underlying mathematical model that is not or partially covered in the data set. In other words, it is natural to require DNN to be aware of the underlying mathematical models (or discretizations) in order for it to be a *reliable and interpretable tool* for sciences and engineering applications. Indeed, we have shown that it is not clear if inverse solutions using purely data-driven DL methods are interpretable. We have presented several model-constrained deep learning approaches—using both feed-forward DNN and autoencoders—to learn inverse solutions while being constrained by the forward model under consideration. The first order optimality conditions show that the proposed model-constrained DL approaches, thanks to the model constraints, provide interpretable inverse solution. In particular, they can provide consistent or equivalent inverse solutions of the original inverse problems. Ongoing work is to investigate the second order optimality conditions and to extend the result to nonlinear inverse problems.

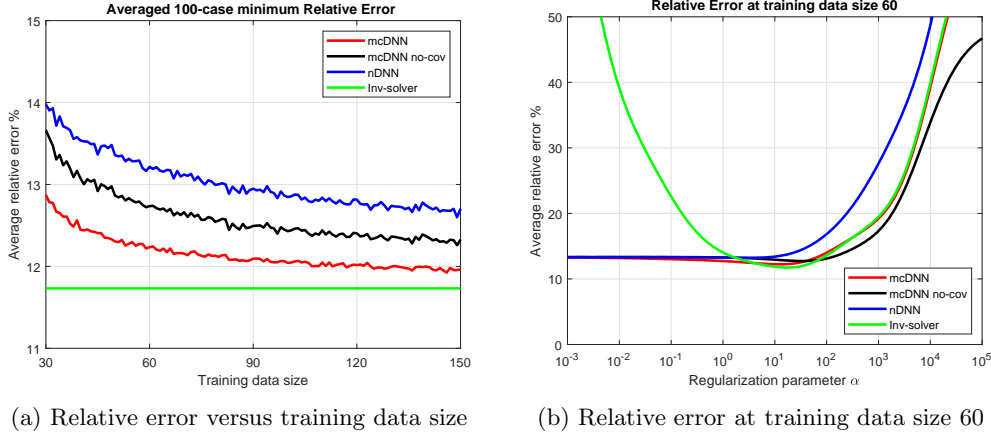


Fig. 1: Average relative error over 100 cases, Dirichlet boundary prior

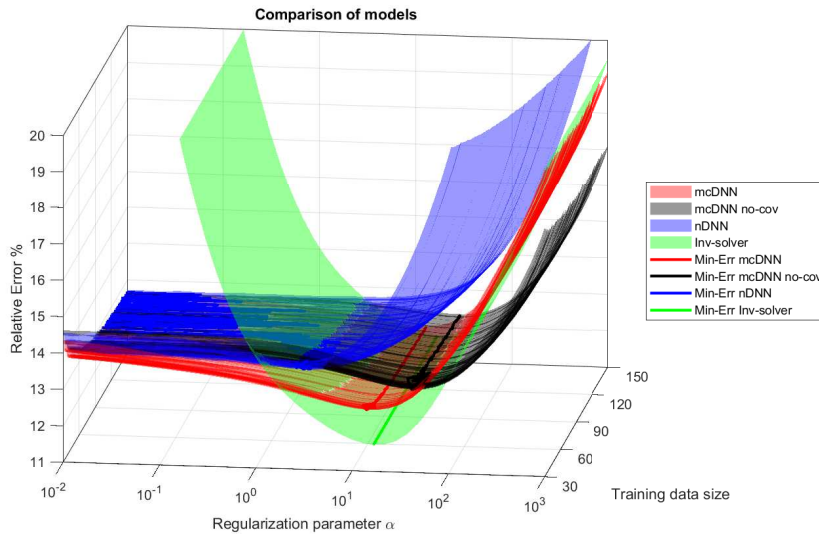


Fig. 2: 3D plot of average relative error over 100 cases, Dirichlet boundary prior

Acknowledgments. The authors would like to thank Sheroze Sheriffdeen, Jonathan Wittmer, Hwan Goh, and Co Tran for fruitful discussions.

REFERENCES

- [1] O. M. Alifanov. *Inverse Heat Transfer Problems*. Springer Verlag, Berlin, Heidelberg, New-York, 1994.
- [2] Christopher M. Bishop. *Pattern Recognition and Machine Learning (Information Science and Statistics)*. Springer-Verlag, Berlin, Heidelberg, 2006.
- [3] Pavel Bochev and Max Gunzburger. *Least-Squares Finite Element Methods*, volume 166. 01 2006.

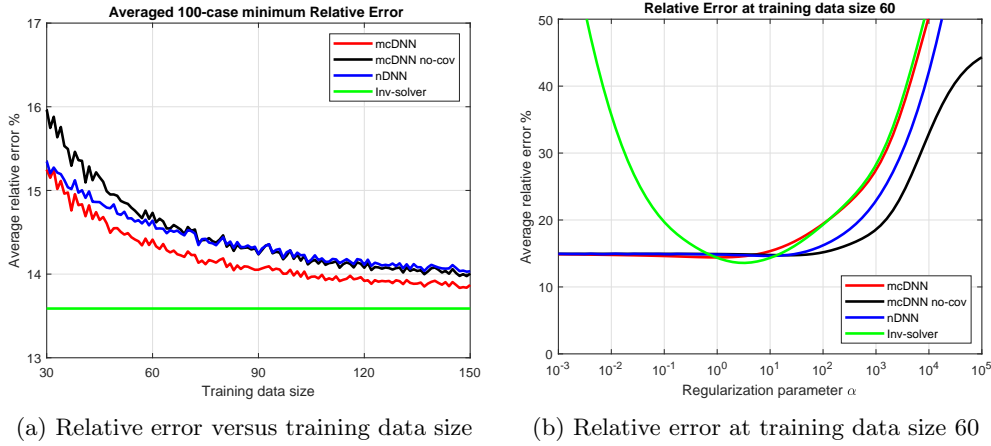


Fig. 3: Average relative error over 100 cases, Relax boundary prior

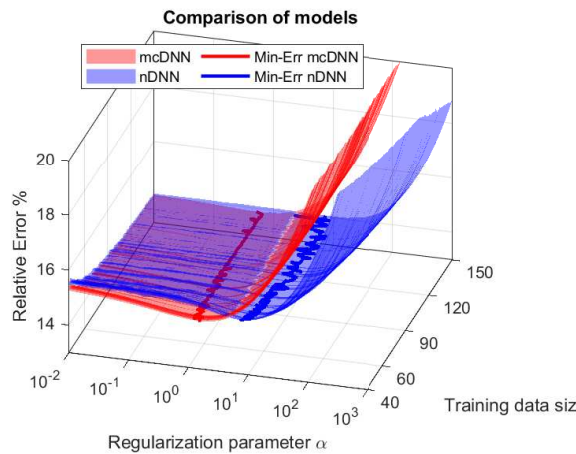


Fig. 4: 3D plot of average relative error over 100 cases, Relax boundary prior

- [4] S. C. Brenner and L. R. Scott. *The Mathematical Theory of Finite Element Methods*. Springer Verlag, Berlin, Heidelberg, New York, second edition, 2002.
- [5] Tan Bui-Thanh, Carsten Burstedde, Omar Ghattas, James Martin, Georg Stadler, and Lucas C. Wilcox. Extreme-scale UQ for Bayesian inverse problems governed by PDEs. In *SC12: Proceedings of the International Conference for High Performance Computing, Networking, Storage and Analysis*, 2012. Gordon Bell Prize finalist, <http://users.ices.utexas.edu/%7Etanbui/PublishedPapers/sc12.pdf>.
- [6] Yuyao Chen, Lu Lu, George Em Karniadakis, and Luca Dal Negro. Physics-informed neural networks for inverse problems in nano-optics and metamaterials. *Opt. Express*, 28(8):11618–11633, Apr 2020.
- [7] P. G. Ciarlet. *The finite element method for elliptic problems*, volume 40 of *Classics in Applied Mathematics*. SIAM (SIAM), Philadelphia, PA, 2002. Reprint of the 1978 original [North-Holland, Amsterdam; MR0520174 (58 #25001)].
- [8] G. Cybenko. Approximation by superpositions of a sigmoidal function. *Mathematics of Control, Signals and Systems*, 2(4):303–314, Dec 1989.

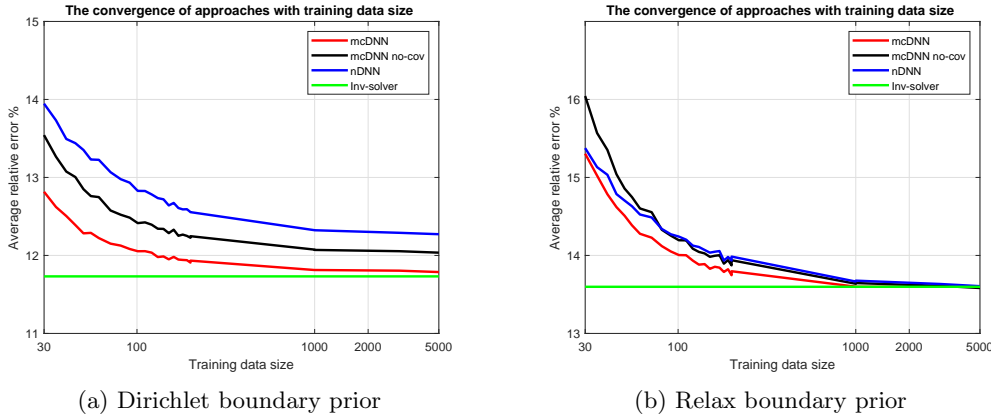


Fig. 5: The convergence rate versus training data size

- [9] Alexandre Ern and Jean-Luc Guermond. *Theory and Practice of Finite Elements*, volume 159 of *Applied Mathematical Sciences*. Springer-Verlag, 2004.
- [10] Hwan Goh, Sheroze Sheriffdeen, and Tan Bui-Thanh. Solving forward and inverse problems using autoencoders, 2019.
- [11] Ian Goodfellow, Yoshua Bengio, and Aaron Courville. *Deep Learning*. MIT Press, 2016. <http://www.deeplearningbook.org>.
- [12] Sepp Hochreiter, Yoshua Bengio, Paolo Frasconi, and Jürgen Schmidhuber. Gradient flow in recurrent nets: the difficulty of learning long-term dependencies, 2001.
- [13] Kurt Hornik, Maxwell Stinchcombe, and Halbert White. Multilayer feedforward networks are universal approximators. *Neural networks*, 2(5):359–366, 1989.
- [14] Jiaqi Jiang, Mingkun Chen, and Jonathan A. Fan. Deep neural networks for the evaluation and design of photonic devices. *Nature Reviews Materials*, Dec 2020.
- [15] Jesse Johnson. Deep, skinny neural networks are not universal approximators. In *International Conference on Learning Representations*, 2019.
- [16] Jari Kaipio and Erkki Somersalo. *Statistical and Computational Inverse Problems*, volume 160 of *Applied Mathematical Sciences*. Springer-Verlag, New York, 2005.
- [17] Keisuke Kojima, Bingnan Wang, Ulugbek Kamilov, Toshiaki Koike-Akino, and Kieran Parsons. Acceleration of fdtd-based inverse design using a neural network approach. In *Advanced Photonics 2017 (IPR, NOMA, Sensors, Networks, SPPCom, PS)*, page ITu1A.4. Optical Society of America, 2017.
- [18] Dimitri Komatsitsch, Jeroen Ritsema, and Jeroen Tromp. The spectral-element method, Beowulf computing, and global seismology. *Science*, 298:1737–1742, 2002.
- [19] Gitta Kutyniok, Philipp Petersen, Mones Raslan, and Reinhold Schneider. A theoretical analysis of deep neural networks and parametric pdes, 2020.
- [20] Matthieu Lefebvre, Ebru Bozda, Henri Calandra, Judy Hill, Wenjie Lei, Daniel Peter, Norbert Podhorszki, David Pugmire, Herurisa Rusmanugroho, James Smith, and Jeroen Tromp. A data centric view of large-scale seismic imaging workflows. *Supercomputing (SC) 13*, 2013. Invited paper.
- [21] Dianjing Liu, Yixuan Tan, Erfan Khoram, and Zongfu Yu. Training deep neural networks for the inverse design of nanophotonic structures. *ACS Photonics*, 5(4):1365–1369, 2018.
- [22] Lu Lu, Xuhui Meng, Zhiping Mao, and George Em Karniadakis. Deepxde: A deep learning library for solving differential equations. *SIAM Review*, 63(1):208–228, 2021.
- [23] Lu Lu, Raphael Pestourie, Wenjie Yao, Zhicheng Wang, Francesc Verdugo, and Steven G. Johnson. Physics-informed neural networks with hard constraints for inverse design, 2021.
- [24] Zhou Lu, Hongming Pu, Feicheng Wang, Zhiqiang Hu, and Liwei Wang. The expressive power of neural networks: A view from the width. In I. Guyon, U. V. Luxburg, S. Bengio, H. Wallach, R. Fergus, S. Vishwanathan, and R. Garnett, editors, *Advances in Neural Information Processing Systems*, volume 30. Curran Associates, Inc., 2017.
- [25] Jie Luo, Xun Li, Xinyuan Zhang, Jiajie Guo, Wei Liu, Yun Lai, Yaohui Zhan, and Min Huang. Deep-learning-enabled inverse engineering of multi-wavelength invisibility-to-

superscattering switching with phase-change materials. *Opt. Express*, 29(7):10527–10537, Mar 2021.

[26] Mehryar Mohri, Afshin Rostamizadeh, and Ameet Talwalkar. *Foundations of Machine Learning*. The MIT Press, 2012.

[27] Dean S. Oliver, Albert C. Reynolds, and Ning Liu. *Inverse theory for petroleum reservoir characterization and history matching*. Cambridge University Press, 2008.

[28] Guofei Pang, Lu Lu, and George Em Karniadakis. fpinns: Fractional physics-informed neural networks. *SIAM Journal on Scientific Computing*, 41(4):A2603–A2626, 2019.

[29] Raphaël Pestourie, Youssef Mroueh, Thanh V. Nguyen, Payel Das, and Steven G. Johnson. Active learning of deep surrogates for pdes: application to metasurface design. *npj Computational Materials*, 6(1):164, Oct 2020.

[30] John Purifoy, Yichen Shen, Li Jing, Yi Yang, Fidel Cano-Renteria, Brendan G. DeLacy, John D. Joannopoulos, Max Tegmark, and Marin Soljačić. Nanophotonic particle simulation and inverse design using artificial neural networks. *Science Advances*, 4(6), 2018.

[31] M. Raissi, P. Perdikaris, and G.E. Karniadakis. Physics-informed neural networks: A deep learning framework for solving forward and inverse problems involving nonlinear partial differential equations. *Journal of Computational Physics*, 378:686 – 707, 2019.

[32] M. Raissi, P. Perdikaris, and G.E. Karniadakis. Physics-informed neural networks: A deep learning framework for solving forward and inverse problems involving nonlinear partial differential equations. *Journal of Computational Physics*, 378:686–707, 2019.

[33] Maziar Raissi and George Em Karniadakis. Hidden physics models: Machine learning of nonlinear partial differential equations. *Journal of Computational Physics*, 357:125 – 141, 2018.

[34] Maziar Raissi, Paris Perdikaris, and George Em Karniadakis. Machine learning of linear differential equations using gaussian processes. *Journal of Computational Physics*, 348:683 – 693, 2017.

[35] Maziar Raissi, Paris Perdikaris, and George Em Karniadakis. Physics informed deep learning (part ii): Data-driven discovery of nonlinear partial differential equations. *arXiv preprint arXiv:1711.10566*, 2017.

[36] Shai Shalev-Shwartz and Shai Ben-David. *Understanding Machine Learning: From Theory to Algorithms*. Cambridge University Press, USA, 2014.

[37] Sunae So, Trevon Badloe, Jaebum Noh, Jorge Bravo-Abad, and Junsuk Rho. Deep learning enabled inverse design in nanophotonics. *Nanophotonics*, 9(5):474, February 2020.

[38] Mohammad H. Tahersima, Keisuke Kojima, Toshiaki Koike-Akino, Devesh Jha, Bingnan Wang, Chungwei Lin, and Kieran Parsons. Deep neural network inverse design of integrated photonic power splitters. *Scientific Reports*, 9(1):1368, Feb 2019.

[39] Albert Tarantola. *Inverse Problem Theory and Methods for Model Parameter Estimation*. SIAM, Philadelphia, PA, 2005.

[40] Rohit K. Tripathy and Ilias Bilionis. Deep uq: Learning deep neural network surrogate models for high dimensional uncertainty quantification. *Journal of Computational Physics*, 375:565 – 588, 2018.

[41] Daniel A. White, William J. Arrighi, Jun Kudo, and Seth E. Watts. Multiscale topology optimization using neural network surrogate models. *Computer Methods in Applied Mechanics and Engineering*, 346:1118–1135, 2019.

[42] Yibo Yang and Paris Perdikaris. Adversarial uncertainty quantification in physics-informed neural networks. *Journal of Computational Physics*, 2019.